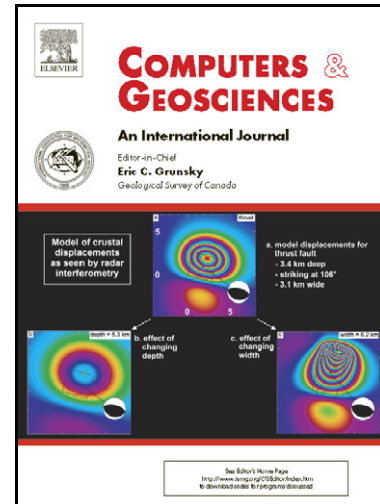# Author's Accepted Manuscript

Construction of accurate geological cross-sections along trenches, cliffs and mountain slopes using photogrammetry

Santiago Martín, Hodei Uzkeda, Josep Poblet, Mayte Bulnes, Ramón Rubio

Cite this article as: Santiago Martín, Hodei Uzkeda, Josep Poblet, Mayte Bulnes and Ramón Rubio, Construction of accurate geological cross-sections along trenches, cliffs and mountain slopes using photogrammetry, *Computers & Geosciences,* http://dx.doi.org/10.1016/j.cageo.2012.09.014

Construction of accurate geological cross-sections along trenches, cliffs and mountain slopes using

photogrammetry

Santiago Martín[1], Hodei Uzkeda[2,*], Josep Poblet[2], Mayte Bulnes[2]; Ramón Rubio[1]

[1] *Departamento de Construcción e Ingeniería de Fabricación, Universidad de Oviedo, Campus de Viesques, Edificio Departamental nº6, 33203 Gijón, Spain, e-mail: martinsantiago@uniovi.es (Martín); rrubio@uniovi.es (Rubio)*

[2] *Departamento de Geología, Universidad de Oviedo, C/Jesús Arias de Velasco s/n, 33005 Oviedo, Spain. E-mail (Uzkeda): hodei@geol.uniovi.es, e-mail (Bulnes): maite@geol.uniovi.es, e-mail (Poblet): jpoblet@geol.uniovi.es*

* Corresponding autor. Tel.: +34 958 103120. Fax: +34 985 103103

Abstract

This paper discusses the application of close range photogrammetry for the construction of geological cross-sections from outcrops located on trenches, cliffs and mountain slopes. Our methodology is based on stereoscopic pairs of photographs of the outcrops on which geological interpretations may be carried out directly using a digital stereo viewer. It is also possible to automatically obtain point clouds. Through control points of known coordinates taken on the field and located in the photographs, the three-dimensional model recovered is correctly geo-referenced and the residual error is minimized. Layers and tectonic structures recognized in the photographs can be easily projected in any desired direction, as, for example, in the direction of

1

the fold axes to obtain a proper view of the geometry of the structures, or in one direction parallel to the tectonic transport vector if a restoration is demanded. The application of this methodology is shown by constructing a detailed geological cross-section at the cliffs of La Conejera Inlet (Asturias, Spain). The studied structures, involving Jurassic rocks, are located in a Permian-Mesozoic extensional basin called Asturian Basin (NW Iberian Peninsula). This basin was partially formed during the opening of the Bay of Biscay and partially inverted during a Cenozoic contraction responsible for the Pyrenees and its western prolongation along the north margin of the Iberian Peninsula.

Keywords: geological cross-section, photogrammetry, stereoscopic pair, photogeological interpretation, structure from motion (SFM)

1. Introduction

The construction of geological cross-sections is one of the most widely used techniques to represent the geometry of the rocks. They are also used to quantify some geological parameters or processes. Both the visualization of the rocks configuration and the quantification of values associated with them have an interest, not only from a purely scientific point of view, but also from an economical one, in those cases where the rocks host geological resources or certain types of human activities. They are also socially relevant in those areas likely to be affected by geological hazards.

From the above, it is clear the importance of constructing a geometrically correct and as much accurate as possible geological cross-section. Apart from human aspects such as the

experience of the geologists, fundamental factors conditioning the precision of the sections are: the quality, the distribution and the abundance of geological data and the techniques used for construction.

The information needed to construct geological cross-sections can come from various sources, the most common would be: surface data (fieldwork, geological maps, photographs), subsurface data (well logs, geophysical methods) and three-dimensional (or pseudo three-dimensional) models (photogrammetry, laser scanning).

In particular, the construction of geological cross-sections from outcrops located on trenches, cliffs and/or mountain trenches poses specific problems. These areas are often not well represented on topographic maps or aerial images because of being highly inclined or vertical. Another issue with this kind of outcrops is their slenderness which makes difficult to maintain the correct proportions all along their route, and may provoke the accumulation of errors. Furthermore, the cliffs usually have an irregular morphology which makes difficult to obtain a complete and proper vision of the outcrop. The geological cross-sections derived from outcrops located in such regions have been prepared using basically four techniques, or combinations of them: directly in the outcrop (freehand drawing); interpreting geologically conventional photographs; obtaining coordinates of points along elements of interest using total stations or laser rangefinders (Xu et al., 2001); creating cloud points using a terrestrial laser scanner (Buckley et al., 2008).

This paper presents a strategy for construction of geological cross-sections, based on photogrammetry, applicable to any type of deformed rocks and tectonic regime under both superficial and deep conditions. It is especially useful when the information comes from rock outcrops located along trenches, cliffs and/or mountain slopes. This procedure consists of: 1) obtaining pairs of overlapping photographs, 2) acquiring geo-referenced checkpoints and locating them in the photographs, 3) processing of these images in order to form stereoscopic pairs, 4) viewing and performing a geological interpretation with a digital stereo viewer, and 5) projecting the photo-geological interpretation onto the geological

section chosen (Fig. 1). Our approach does not require the extraction of point clouds, meshes or textures which greatly simplifies the process.

In our view, the use of this method improves some of the weaknesses of the techniques mentioned above. For instance, it prevents the gross distortion caused by the difficulty of preserving the scale of the elements represented when freehand drawing or due to the distortion of the pictures themselves (especially in their edges). Furthermore, these two methods only allow the construction of the geological cross-section on the surface of outcrop so, if it is oblique to the structures, it cannot display their true geometry. The situation may get even more complicated if the outcrop shows entrants and salients or changes of direction. On the contrary, the method described in this paper corrects automatically any distortion in the geological interpretation and the result may be projected onto a chosen geologically meaningful plane. The use of total stations or laser rangefinders implies that only data related to the selected points are stored. While in our method additional data can be obtained quickly and simply in the laboratory, simply by displaying and interpreting again new parts of the photographs. Furthermore, the point-by-point capture may be too time-consuming if a lot of points are needed. Three-dimensional scanning provides a huge volume of data (points with coordinates XYZ and colour if it is combined with a camera) but only a small portion (lines defined by the intersection of beds or structural elements with the topographic surface) will be used when constructing the cross-section. Photogrammetric techniques are capable of getting similar point clouds as well, but with the additional advantage of offering the chance of getting stereoscopic pairs. A stereoscopic viewer allows the visualization of the outcrops in proper three dimensions, almost as working directly in the field, and the extraction of three-dimensional coordinates of only the chosen points. Moreover, digital photographic cameras are obviously less expensive than a terrestrial laser scanner.

Those benefits are the reason why photogrammetry techniques have been used in geology, mainly on mapping from aerial of satellite images (e.g., Berger et al., 1992; Lebel and Da Roza, 1999), but also

4

in studies using terrestrial photographs (Dueholm et al., 1993; Haneberg, 2008; Rieke-Zapp et al., 2009, amongst others).

2. Fundamentals of photogrammetry

Any photogrammetric method requires solving four main problems: image acquisition, camera calibration (interior parameters), resection (exterior parameters) and intersection.

Camera calibration and resection might be solved as two different problems or as a single one using the bundle adjustment method (Triggs et al., 2000). The mathematical basis of the camera calibration is the pinhole camera model which describes the relationship between the coordinates of a three-dimensional point and its projection onto the image plane of an ideal pinhole camera. However, this is a simplification of the actual optical geometry of a digital camera, because not only the focal length and the coordinates of the centre of projection must be known, but also the distortion coefficients of the lens. Usually two radial and three tangential coefficients are enough to calibrate a camera. These parameters may be calculated using a calibration object, as, for instance, a chessboard (Bradski and Kaehler, 2008). Resection is the process of calculating the exterior orientation parameters: translation and rotation matrixes between each two camera positions. The basic geometry of a stereo system (the simplest case) is referred to as epipolar geometry. In order to resolve the problem a set of correspondence points in both photographs, called target or control points, are needed. If there are not available three-dimensional coordinates of them the issue may be overtaken but the translation matrix will not preserve the actual scale of the objects depicted in the pictures. Although some mathematical formulations can find a solution to the problem with only five non-colinear targets, in practice, at least eight points are used (Ma et al., 2004). If the three-dimensional coordinates of the targets were known (for example, by using a

5

differential GPS) only three correspondence points would be required. The use of more than three points of known coordinates allows the improvement of the previous camera calibration results.

The last issue to be worked out is the intersection. Having two homologous projected points in two images calibrated and orientated, the collinearity equations are used to retrieve the three-dimensional coordinates of the object point. Relative simple image processing techniques (Gonzalez and Woods, 2008) can be utilized to find correspondence points between two images once they are oriented, as the epipolar geometry implies that the search is restricted to the epipolar lines, i.e. is a one-dimensional instead of a two-dimensional search.

Two final products may be achieved with the stereo photogrammetry: a point cloud of the object and coplanar stereoscopic pairs that can be visualized and posteriorly interpreted.

This second technique is based on the stereoscopic vision of human beings to, from pairs of flat digital images, recreating a three-dimensional model of the photographed object in the mind of the observer (Lerma García, 2002). As the photographs of each pair have been taken from different positions and each one is observed separately for each eye, so that two slightly different images are transmitted to the brain and interpreted as differences in depth.

The peculiar characteristics of the problem faced in this work, slender outcrops that runs along several hundreds of metres, prevent the recovery of multiple convergent takes around the three-dimensional model. In other projects it is viable to rotate around the object of interest getting enough pictures to solve the difficulties associated to the camera calibration and resection via a bundle strategy as previously mentioned. The fact that it is not possible to rotate all around a cliff closing the takes, i.e. ending where the first photograph was taken, supposes that the possible errors would accumulate progressively from one end to the other one of the model. This could be a limitation because the bundle adjustment presents, in general, a better accuracy. However, if the extrinsic calibration (resection) is made working with points of known three-dimensional coordinates, the mathematical methods employed allow

6

the refinement of the initial intrinsic calibration and, subsequently, improving the final result. So that, the

traditional stereo photogrammetric method, based on the recovery of the three-dimensional model through

independent stereoscopic pairs, is recommended for this project.

3. Proposed methodology

The implementation of the strategy presented in this paper comprises five different stages.

3.1 Getting stereo pairs of photographs

The images are typically acquired using cameras with fixed-focus lens, given that they have less

optical deformation than those with zoom and that the camera calibration remains more stable during the

whole project. It is desirable to work with large depths of field (DOF) to ensure a sharp vision of the

entire image, which, in turn, means increasing the f-number and decreasing the aperture diameter. Typical

values are f/11 or f/16. An unfortunate consequence of this it is a reduction in the amount of light

transmitted so longer exposure times are necessary and a tripod mandatory. By using large DOF

photographs for the entire project the camera calibration will remain more stable. Moreover, as large DOF

increases the sharpness, it improves the image processing techniques used to find correspondence points.

The pictures obtained will preserve better the details, both in the shaded and the highlighted areas,

if HDR (high-dynamic range) technique is used. It consists of capturing several conventional photographs

that are identical except for their exposure value (EV) and merging them to a single HDR picture (Mann

and Picard, 1995). The idea behind HDR is getting a picture where each zone is visualized with the most

suitable exposure, for example, the darker sectors will be selected from the primary picture taken with the higher EV so they appear lightened enough to detect their details. Three different shots are sufficient, one with the "correct" exposition, a second one underexposed to capture highlights, and a third one overexposed to record the shaded regions. The fusion can be done with standard image processing software. A similar result may be obtained working with raw digital format. It is faster in the field only one shot for each photograph is required) but it also involves a processing in the laboratory with specialised software.

We recommend taking the photographs in independent pairs, shooting both of each couple with parallel axes and perpendicular to the outcrop (Figure 2). These cautions are of great help when carrying out the rectification and construction of epipolar images. A last comment must be done about the sun lighting when acquiring the photographs. In spite that the HDR techniques may solve part of the shadows and highlights issues, it is better to avoid shooting against the Sun. This can be done, for example, taking the pictures in the morning when working on east facing outcrops or in the evening at west facing outcrops. Another way to minimize the effects of the sun light is to take the photographs on cloudy days.

The distance between the object and the camera affects the width and height resolution (which would be the pixel size on the outcrop) achieved, while the distance between the cameras from one picture to the following (baseline) is related to the depth resolution. The width and height resolutions can be obtained by the following expression:

$$r_p = d / f$$

where r_p is the resolution in mm/pixel, d is the shooting distance in mm and f is the focal length of the camera in pixels (Table 1). The depth resolution may be calculated with the expression:

$$r_z = d^2 / (f \cdot s)$$

where r_z is the depth resolution in mm/pixel, d the shooting distance in mm, f the focal length of the camera in pixels and s the baseline in mm (Table 1). In general, the larger the displacement, the smaller the uncertainty in depth (better resolution), but also less overlap which implies more pairs for each zone. A compromise must be reached between these two factors.

3.2 Acquisition of control points

In addition to the photographs, measurements of control points must be done in the field. It is necessary to geo-reference a number of correspondence control points for each couple of photographs that will form a stereoscopic pair. This way the resection can be done and the intrinsic calibration may be improved. It allows also joining the geological interpretations made at different stereoscopic pairs. Theoretically with three points should be enough but the results will be better if more points are taken. For this step we used a total station and differential GPS to capture about eight points per pair. These points should lie in the overlapping fringe of both photographs and be distributed as evenly as possible throughout the entire common area. In cases where the trenches, cliffs or mountain slopes are highly irregular it is advisable to take measurements of a greater number of points, trying to place them at the diverse planes that may exist, for example, two cliff faces at different depths. The control points may be either natural points or targets placed there purposely. The quickness for the record of the control points, as well as for the processing of the photographs and the accuracy of the results, increases with the targets, that should be of bright colours with high contrast between quadrants (the recommended pattern for the target vary depending on the software employed, it may be alternate quadrants or circular sectors) and with the outcrop colour and be small to obscure the minimum surface, but big enough to be identifiable in the field (in our experience about 40x40 pixels in the picture is enough). But, this approach has its own

9

disadvantages as would be that the targets will appear in the stereoscopic pairs and that when working with large outcrops might be impossible to distribute them adequately.

3.3 Intrinsic and extrinsic calibration

The photographs that will constitute stereoscopic pairs should be taken with a digital single-lens reflex camera that has been, or will subsequently be, calibrated. It is recommended using a fixed optical model to avoid any difference between the time of photographing and calibration. The camera calibration is a necessary process that allows knowing the focal, the centre of projection and the distortion coefficients of the photographic device. These parameters are essential when processing the photographs which will become stereo pairs. There are several methods to perform the calibration. A widespread one consists of taking a series of photographs from different positions of a planar pattern (i.e. a chessboard pattern). With this information the necessary parameters may be calculated using in-house developed software (called Stereo Rectification, see the website www.ideascad.es for further information) which uses the OpenCV (Open Source Computer Vision) library (Bradski and Kaehler, 2008). This library has been developed by Intel and it is mainly aimed at real time computer vision.

The resection is made using the control points captured in the field and with the same in-house software employed before for the intrinsic calibration. The utilization of targets as control points allows the recovery of the pixel coordinates of these markers with sub-pixel accuracy via interpolation (Fig. 3a). In case that natural control points are used the software permits a refinement of the manual picks through a SAD algorithm (Sum of Absolute Differences) (Fig. 3b). A measurement of the error introduced may be obtained comparing the three-dimensional coordinates recorded for the control points with the total station, with those recovered from the three-dimensional model. It can also help to highlight aberrant

points caused, for example, by mistakes when employing the total station during its acquisition. These points should not be included for the rectification.

Reached this point it is possible to generate point clouds that may be geo-referenced and exported with associated colour information (XYZ + RGB) to different formats (TXT, PLY, OBJ). It is also feasible to create a stereo pair to be visualized in a stereoscopic viewer. This requires that the two images align exactly. Unfortunately, a perfectly aligned configuration is rare with an actual stereo system, since it is virtually impossible that the two cameras have exactly coplanar, row-aligned imaging planes. So, it is compulsory to make the stereo rectification which implies reprojecting the image planes of our two cameras so that they reside in the exact same plane, with image rows perfectly aligned into a frontal parallel configuration (i.e., epipolar configuration). The result is two rectified photographs (Fig. 4) ready to be visualize and interpreted geologically.

3.4 Visualization and interpretation of the stereo pairs

The visualization of the stereo pairs and the geological interpretation (i.e. manual extraction of three-dimensional polylines) were carried out working with VISAGE, an in-house software (Martín et al., 2007) based on the open source library GLSVe (Martín et al., 2011) developed by the same team. The vision of the photographs with the shutter glasses is excellent, but no matter what good it may be, there are still some geological features which are better seen in the field. So, even though the software provides tools to make the complete geological interpretation on the screen it is advisable to find them on interpretations, schemes, etc. done directly in the field. This procedure is especially helpful when there are small-scale structures or regions where the photographs are not of great quality (shadows, oclussions, etc.). The users may introduce a new source of error when interpreting that will depend on their stereoscopic visual acuity. Anyhow, it should not be greater than a pixel.

When the stereo pair is interpreted (Fig. 5), the polylines may be exported to different formats (TXT, DXF) and geo-referenced. The geo-referencing enables putting all of them together and obtaining an interpretation of the geology of the study area without any photographic distortion. Once this has been done, it is time to take the final step and construct the cross-section projecting the extracted polylines onto a geologically relevant plane. Before performing this action it is desirable to filter the lines to prevent duplicities where two consecutive pairs of photographs overlap.

3.5 Projection of the geological interpretation onto the selected plane

The goal of this stage is to project the three-dimensional geological interpretation onto a plane, what implies transforming the three-dimensional coordinates in two-dimensional.

First the strike of the geological cross-section must be chosen; commonly, the direction selected is perpendicular to the fold axes and parallel to the direction of tectonic transport vector. The most basic principle that must be borne in mind when projecting the data in folded regions is the geometry of the fold axes. This geometry can be known from field observations and data analysis techniques based on stereographic projection (see for example Ramsay and Huber, 1987). In the case of cylindrical structures the projection vector should be the fold axis. The distance of projection up to which is reasonable to project the data depends on the cylindricality degree of the structure along the strike. In occasions non-cylindrical folds can be decomposed into smaller domains of cylindrical geometry (Langenberg et al., 1987). In this case the distance of projection would be defined by the boundaries of each domain. If the structure is clearly conical, the vector of projection for each of the data should be the generatrix corresponding to that point (Bengtson, 1980; DePaor, 1988; Groshong, 1999). When projecting data of such type of folds it must be taken into account that they do not extend indefinitely but end where the generatrixes converge (Wilson, 1967).

12

4. Application of the method to a cliff: geological cross-section of La Conejera Inlet

To show the usefulness of the described method it has been applied to an actual field example corresponding to an almost continuous outcrop along a cliff. This section is situated in the central-eastern coast of Asturias (Northwest of the Iberian Peninsula) (Fig. 6), in the so-called La Conejera Inlet (La Coneyera in Asturian). It is approximately 225 m long, about 50 m high and is Northwest – Southeast oriented (Fig. 7). Because of its steep slope and its northern orientation the cliff appears properly represented neither in the topographic maps nor in the aerial photographs of the region. This situation makes really complicated to capture the geology visible in the terrain in a geological map. Furthermore, the cliff orientation is oblique to the direction of the main tectonic structures and, subsequently, offers an apparent view (Figs. 7 and 8). Another limiting factor is the dimensions of the outcrop (both the lateral and the vertical extension) which, together with the narrow beach (Fig. 7), prevents getting a good overview of the cliff. This makes virtually impossible to create accurate freehand schemes observing the proportions and/or taking conventional pictures to interpret them in a traditional way. These complexities make the field example from La Conejera Inlet a perfect candidate to be analysed by means of the procedure presented in this work, providing that if the results are satisfactory there will be no doubt that simpler situations (as road trenches) will be no challenge.

4.1 Geological setting

The rocks that constitute the outcrop are part of the Asturian Basin, a sedimentary basin filled by materials with ages ranging from Permian to Cretaceous (Fig. 6) and whose northern portion is offshore.

13

The Permian materials and the lower part of the Mesozoic sediments underwent diverse extensional tectonic episodes from Permian to Early Cretaceous (Lepvrier and Martínez-García, 1990; García-Ramos, 1997) partly related to the opening of the Bay of Biscay situated to the north of the studied zone. These materials, together with later Mesozoic and Cenozoic materials (the latter forming small basins), were deformed by the Alpine contraction caused by the convergence of the Iberian Plate and Eurasia (Late Cretaceous to Cenozoic) (Alonso et al., 1996) which created the Pyrenees and their prolongation along the northern Iberian margin. The tectonic activity suffered by this portion of the Northwest of the Iberian Peninsula has prolonged till the present day as shown by reverse faults that involve Quaternary materials (Gutiérrez-Claverol et al., 2006) or certain seismic activity of small magnitude (López-Fernández et al., 2004). It was in recent times also when the uplift of Quaternary marine abrasion platforms generated cliffs like the one where the present study is carried out (Flor, 1983; Mary, 1983; Álvarez-Marrón et al., 2008, among others).

The Asturian Basin lays unconformably on top of Palaeozoic materials with ages from Cambrian to Carboniferous which belongs to the Cantabrian Zone. This zone is the fold and thrust belt of the Variscan orogeny in the Northwest of the Iberian Peninsula developed from Devonian to Carboniferous times.

4.2 Data Acquisition

The outcrop of La Conejera Inlet was covered with a total of 72 photographs that allowed obtaining 24 HDR images. These photographs were taken with a digital single-lens reflex camera OLYMPUS E-410, with image resolution of 3648 x 3726 pixels, using a ZUIKO DIGITAL 35 mm F3.5 macro lens (focal length equivalent to 70 mm on a 35 mm camera), and working with an f number of 22. The pictures were taken at distances to the cliff varying from 30 to 85 m and baselines from 4 to 15 m.

Thus, the base-to-height ratio ranges from 0.13 to 0.17. This results in width-height resolutions (pixel sizes on the outcrop) ranging from 4.0 to 11.4 mm (Table 2), depth resolutions of 21.9 to 92.0 mm (Table 2), and an overlapping of about 70%. The size of this voxel provides a first estimation of the uncertainty associated with the methodology proposed. No better accuracies than its size should be expected. The positions of 113 natural control points situated on natural features and distributed as evenly as possible across the photographs were captured with a total station (TOPCON GPT-7000) and differential GPS (TRIMBLE 4600 LS) to eventually create 12 stereoscopic pairs (Fig. 3). The nominal accuracy of the GPS (after postprocessing) is of 5 mm in the horizontal and 10 mm in the vertical, a bit worse than that of the total station (2 mm when shooting from more than 25 m).

4.3 Considerations

The rectification of the images should lead to an epipolar configuration with no vertical parallax. However, a slight parallax may remain and can be used as an error measurement; it includes residuals in camera intrinsic and extrinsic calibrations, plus residuals in the determination of the control points. Another estimation of the error committed may be obtained calculating the distance between the position of the control points recorded by the total station and their locations in the extracted three-dimensional model. The quality of the resulting model for our field example will be analysed in detail in the discussion.

The stereoscopic pairs were loaded in the software Visage and later visualized and interpreted with the help of the shutter glasses. The geological interpretation was supported by direct field observations reflected on previously taken paper versions of the photographs. This additional information is: a) interpretation of the geometry of some beds and tectonic structures; b) interpretation of the spatial and temporal relationships between certain structures; and c) measurements of orientation of planar and

linear elements as fold limbs, axial planes, fold axes, fracture surfaces and kinematic elements related to them. Once finished the geological interpretation of the 11 pairs (Fig. 5), the coordinates of the points forming the drawn elements were extracted. A manual filtering was carried out to eliminate those repeated points that had been interpreted on adjacent pairs. The final result, after the assemblage, is a set of lines depicting the different geologic elements identified (stratification and faults) that offer a pretty reliable vision of their disposition in the field.

The fact that the studied region has undergone several tectonic episodes could, initially, imply an additional complication when choosing the plane for the cross-section. Fortunately, the orientation of many of the older extensional structures coincides approximately with the orientation of the younger contractional ones (Fig. 8). There are also evidences that some of the contractional structures correspond to older inherited structures reactivated. The kinematic indicators measured in the field for both the elder normal faults and the reverse ones evidence that, in this region, the tectonic transport vectors of these two episodes are approximately parallel (Fig. 8b) and follow, generally, a direction NNW – SSE. The orientation of the cross-section was determined based on the analysis of fold axes (Fig. 8a) and the disposition of slickensides and other kinematic criteria identified on the surfaces of the main faults (Fig. 8b). The cross-section plane must be as much perpendicular as possible to the maxima of the fold axes populations and must contain the maxima of the kinematic indicators. Two sectors with unequal mean orientations of the fold axes were separated: one to the NW whose mean orientation is 243/04; and another one to the SE whose mean direction is 268/02. Since the structures have a cylindrical character, as the π diagrams (Ramsay, 1967) show (Fig. 8), the northwestern sector was projected onto a plane oriented N027W, 86NE following the mean direction of the fold axes, whereas the other was projected onto a plane oriented N002W, 88E. Both section planes are perpendicular to the identified fold axes within each of the sectors (Fig. 9) and adjust quite properly to a plane fitting the slickensides (Fig. 10). The resulting planes show certain obliquity to the cliffs. Their spatial positions were selected close to the rock wall trying to minimize the distance for the data projection (Fig. 11). Eventually, both cross-sections were

combined to provide a view of the whole structure; the result is shown in fig. 12. The joining of both sections was made through the inflection line existent between two adjacent folds (an anticline in the NW section and a syncline in the SE section).

4.4 Main geological features of La Conejera Inlet

The rocks that appear at the cliffs of La Conejera Inlet belong to the Members Buerres (lower member) and Santa Mera (upper member) of the Rodiles Formation (Valenzuela et al., 1986), with an age Early to Middle Jurassic (Suárez Vega, 1974). This formation consists basically of an alternation of marls and limestones, being the latter more abundant in the lower member. These rocks are affected by folds and normal, reverse and strike- faults, of diverse dimensions and orientations (Fig. 12), as well as by other structures such as joints and tension gashes.

The main structures at the cliffs of La Conejera Inlet are two normal faults of decametre-scale, at least their outcropping portion, that limit a sector where deformation is concentrated (Fig. 12). The northwesternmost main fault, has a strike approximately NE-SW and dips around 65º to 75º to the SE. The southernmost main fault shows a strike almost parallel to the former and its dip ranges from 45º to 80º to the NW. Though both faults separate the Santa Mera Member, in the hangingwall, from the Buerres Member, in the footwall, the displacement is greater along the northwestern one. This has been deduced using one key bed that corresponds, roughly, to the Sinemurian – Pliensbachian boundary. In outline, the cross-section illustrates the hangingwall of an asymmetrical graben structure. The geometry of the beds in the hangingwall of both main faults, with sub-horizontal strata at the southern end that pass to moderately dipping beds towards the northern fault, could be interpreted as a rollover anticline associated with that fault. Therefore, it is possible that the main northern fault has listric geometry at depth, or a planar geometry linked to a deep detachment. It is in the hangingwall where most of the deformation occurred,

however, its distribution along this block is not uniform. There is a gradual transition from its southern

border to the northern one, passing from a region subtly deformed to another with beds inclined

moderately to the NW and rather deformed by a large number of minor faults and folds. Thus, the amount

of deformation seems to increase in the hangingwall analogously to the general stratification dip; it is

greater towards the northern main normal fault. This special distribution, together with the fact that the

deformation of compressive type (reverse faults and related folds) is restricted to the hangingwall of the

main normal faults, leads to think that these faults would have caused a buttressing effect during a

contractional event that took place after their activity as normal faults. The two deformational processes

identified in the field are in accordance with the regional setting where an extensional episode (related to

the opening of the Bay of Biscay) and a latter compressional one (Pyrenees formation) took place.

5. Discussion, considerations about the proposed methodology

The final result of the process outlined here is a geological cross-section projected onto a selected

plane. Since it is not possible to rotate all around the cliff closing the takes, the section was made by

joining several interpretations of independent stereoscopic pairs. It is possible to get an estimation of the

errors committed for each pair. There are two main factors to take into account: difference between the

coordinates of the control points measured with the GPS and the total station and those calculated by

photogrammetry, and the residual vertical disparities after the rectification (Table 2). The detection of

control points with high discrepancies in their three-dimensional coordinates and/or great vertical

disparities may help finding aberrant points. Results shown in Table 2 do not include those points, which

were removed from the project before solving the stereo rectification problem. Only one point was

excluded due to its high three-dimensional discrepancy (above 50 centimetres), while seven points were

discarded because vertical disparities (above 3 pixels).

18

Another fact to consider is the three-dimensional resolution of the method, which is function of the camera digital sensor density of pixel, the shooting distance and the distance between the cameras in each stereo setup. The two first parameters control the XY (perpendicular to shooting axis) resolution, while the latter one is related to the Z (depth) resolution. The coordinates of any three-dimensional point recovered will lie inside a voxel whose XYZ dimensions represent the uncertainty of the technique. The first column of Table 2 shows the voxel dimensions for the configuration of each pair.

To get a correct comprehension of the importance of the errors it is crucial to keep in mind the scale at which we are working. In the case of La Conejera Inlet the cross section extends for more than 200 m and an adequate view of the whole structure may be achieved interpreting just one bed for each metre of the stratigraphic column. Given this, errors of centimetre-scale should not suppose a big issue for the interpretation made.

Observing the predicted voxel sizes (Table 2) the greatest uncertainties come from the depth (Z) dimension, which can reach a value close to 10 centimetres (pair 11), although typically is around 5 cm. The width-height resolution (XY) is, in the worst of the cases, of about only 1 cm.

It is convenient to state the misfit of the exterior orientation model. To do that we compared the coordinates of the targets measured via the total station (targets used in the exterior orientation procedure) and the coordinates of the same targets recovered from the photogrammetric model. The root-mean-square deviation (RMSD) is slightly smaller than 16 cm (Table 2) with an average absolute deviation of about 5 cm. Analysing pair by pair (sorted from Northwest to Southeast), the greatest errors appear in pairs 1, 5 and 9, being more or less of 20 cm with average deviations ranging from 5 (pair 1) to 8 (pairs 5 and 9) cm. As expectable the discrepancies are greater, though not excessively (except for pair 1), than the voxel diagonal. Their means range from 3.7 (pair 5) to 1.3 (pair 3) times the diagonal.

A final evaluation of the quality of the work is done analysing the residual vertical disparities. The results obtained (Table 2) are close to a sub-pixel error, which is considered the limit of modern

photogrammetry. The residual vertical disparity (Table 2) is commonly lesser than 1 pixel, except for four pairs (1, 8, 9 and 12). Two of them (pairs 1 and 9) coincide with those that showed greater discrepancies when comparing the coordinates of their control points. This is something expectable, since worse calibrations (reflected in greater residual disparities) should lead to less accurate models.

The examination of the errors committed for each pair makes us think that the accuracy reached with the methodology proposed is more than enough for the aimed objective (general vision of the structure cropping out at the cliffs of La Conejera Inlet). Of course, more detailed studies of some parts of the structure (i.e., minor folds and faults) would probably require the acquisition of closer photographs (to reduce the voxel size) and a more exhaustive refinement of the control points until reaching acceptable errors for the residual disparities and when comparing the coordinates.

A better result might be achieved using targets instead of natural control points. But, as said before, the height of the cliffs in our example prevents the utilization of such elements.

An interesting fact of the study here presented is the time spent during its realization. The most time-consuming task was the visualization and interpretation of the stereoscopic pairs. This is especially true when using a digital stereoscopic system for the first time as the visualization may be a little tricky. On the contrary, the fieldwork is comparatively faster. The calibration and rectification of the photographs are also pretty immediate. These steps require only identifying the control points and assigning them their coordinates.

So, this procedure allows creating an accurate geological cross-section in a relatively easy and quick way, being the most laborious and slow work the interpretation of the stereo pairs. However, this task is progressively faster as the experience of the geologist with the digital stereoscopic system increases.

6. Conclusions

In this work a strategy to build geological cross-sections using data collected from trenches, cliffs and mountain slopes has been introduced. This methodology relies on photogrammetry and is able to produce geometrically correct geological sections across regions affected by any tectonic regime and with diverse deformation conditions. The greatest advantage of this technique, in relation to others, is that it allows viewing the outcrop in three-dimensions in the laboratory and making a photogeological interpretation without any distorsion and with a correct scale. The interpretation may be projected to any desired plane section. It offers a vision of the whole outcrop, which means that more information may be added to the geological interpretation without needing to return to the field, just by drawing more beds (or structural elements) as required. It also provides a complete vision of the whole structure and of the actual distribution of any smaller-scale element such as minor structures. This allows obtaining information about distances between different elements which can be tricky in situations where the cliff, trench, etc. has a lot of bends. The viability of this method has been proved through its application to a cliff of the Asturian coast (NW Iberian Peninsula) formed by Jurassic materials folded and faulted during the extensional events responsible for the formation of the Asturian Basin and a subsequent contractional episode related to the formation of the Pyrenees and its western prolongation. In spite that the software Visage was initially thought to deal with aerial photographs, in this work we have shown that it can be used satisfactorily also to construct accurate geological cross-sections with terrestrial pictures.

Acknowledgments

We wish to thank Rodrigo Escribano for having initiated us in this research line, Rubén Velasco for his help with computer issues and Isabel Moriano for her collaboration in the field work. The authors

21

References

Alonso, J.L., Gallastegui, J., García-Ramos, J.C. and Poblet, J. (2009): Estructuras mesozoicas y cenozoicas relacionadas con la apertura y cierre parcial del Golfo de Vizcaya (Zona Cantábrica – Asturias) (Mesozoic and cenozoic structures related with the opening and partial closure of the Bay of Biscay (Cantabrian Zone – Asturias)). Field guide 6th Conference of the Atlantic Iberian Margin, 18 pp.

Alonso, J.L., Pulgar, F.J., García-Ramos, J.C. and Barba, P. (1996): Tertiary basins and alpine tectonics in the Cantabrian Mountains. In: Friend, P.F. y Dabrio, C.J. (Eds.) Tertiary Basins of Spain: The Stratigraphic Record of Crustal Kinematics. Cambridge University Press, Cambridge, 214-227.

Álvarez-Marron, J., Hetzel, R., Niedennann, S., Menéndez, R. and Marquínez, J. (2008): Origin, structure and exposure history of a wave-cut platform more than 1 Ma in age at the coast of northern Spain: A multiple cosmogenic nuclide approach. Geomorphology 93, 316-334.

Bengtson, C.A. (1980): Structural uses of tangent diagrams. Geology 8 (12), 599–602.

Berger, Z., Lee Williams, T.H. and Anderson, D.W. (1992): Geologic stereo mapping of geologic structures with SPOT satellite data. American Association of Petroleum Geologists Bulletin 76 (1), 101-120.

Bradski, G. and Kaehler, A. (2008): Learning OpenCV. Computer Vision with the OpenCV Library. O'Reilly Media, Sebastopol, 578 p.

Buckley, S.J., Howell, J.A., Enge, H.D. and Kurz, T.H. (2008): Terrestrial laser scanning in geology: data acquisition, processing and accuracy considerations. Journal of the Geological Society 165 (3), 625-638.

DePaor, D.G. (1988): Balanced section in thrust belts. Part 1: construction. American Association of Petroleum Geologists Bulletin 72 (1), 73–90.

Dueholm, K.S., Garde, A.A. and Pedersen, A.K. (1993): Preparation of accurate geological and structural maps, cross-sections or block diagrams from colour slides, using multi-model photogrammetry. Journal of Structural Geology 15 (7), 933-937.

Flor, G. (1983): Las rasas asturianas; ensayos de correlación y emplazamiento (The asturian wave-cut platforms; correlation and emplacement essays). Trabajos de Geología, 13: 65-81.

García-Ramos, J.C. (1997): La sucesión jurásica de la Cuenca Asturiana: entorno pa-leogeográfico regional y relaciones tectónica-sedimentación (The Jurassic succession of the Asturian Basin: regional paleogeographic setting and tectonics-sedimentation relations). Proceedings 4th Conference of the Jurassic of Spain, Alcañiz, Teruel, 13-14.

Gonzalez, R.C. and Woods, R.E. (2008): Digital Image Processing. Prentice Hall, New Jersey, 976 pp.

Groshong, R.H. (1999): 3-D Structural Geology. Springer-Verlag, Berlin, 324 pp.

Gutiérrez Claverol, M., López-Fernández, C. and Alonso, J.L. (2006): Procesos neotectónicos en los depósitos de rasa en la zona de Canero (Occidente de Asturias) (Neotectonic processes in the wave-cut platform deposits in the zone of Canero (West of Asturias)). Geogaceta 40, 75-78.

Haneberg, W.C. (2008): Using close range terrestrial digital photogrammetry for 3-D rock slope

modelling and discontinuity mapping in the United States. Bulletin of Engineering Geology and

the Environment 67 (4), 457-469.

Langenberg, W., Charleswoth, H. and La Riviere, A. (1987): Computer constructed cross-sections of the

Morcles nappe. Eclogae Geologicae Helvetiae 80 (3), 655–667.

Lebel, D. and Da Roza, R. (1999): An innovative approach using digital photogrammetry to map geology

in the Porcupine Hills, Southern Alberta, Canada. Photogrammetric Engineering & Remote

Sensing 65 (3), 281-288.

Lerma García, J.L. (2002): Fotogrametría Moderna: Analítica y Digital (Modern Photogrammetry:

Analitical and Digital). Publication services of the Universidad Politécnica de Valencia, Valencia,

549 pp.

Lepvrier, C. and Martínez-García, E. (1990): Fault development and stress evolution of the post-

Hercynian Asturian basin (Asturias and Cantabria, northwestern Spain). Tectonophysics 184 (3-

4), 345-356.

López-Fernández, C., Pulgar, J.A., González-Cortina, J.M., Gallart, J., Díaz, J. and Ruíz, M. (2004):

Actividad sísmica en el NO de la Península Ibérica observada por la red sísmica local del

Proyecto GASPI (Seismic activity in the NW of the Iberian Peninsula observed by the local

seismic net of the GASPI Project). Trabajos de Geología 24, 91-106.

Ma, Y., Soatto, S., Kosecka, J. and Sastry, S. (2004): An Invitation to 3-D Vision: From Images to

Geometric Models. Springer-Verlag, Berlin, 526 pp.

Mann, S. and Picard, R.W. (1995): On being 'undigital' with digital cameras: extending dynamic range

by combining differently exposed pictures. Proceedings 48th Annual Conference of the Society

for Imaging Science and Technology, 442-448.

Martín, S., García, S., Suárez, J., Rubio, R., Gallego, R. and Morán, S. (2007): VISAGE: Estereoscopio virtual aplicado a la Geología (VISAGE: Virtual stereoscope applied to Geology). XII International Conference of Energy and Mineral Resources, Oviedo, Asturias.

Martín, S., Pupo, L., Cabrera, Y. and Rubio, R. (2011): An open-source C sharp library based on OpenGL for stereoscopic graphic applications development. Proceedings 1st International Conference on Simulation and Modeling Methodologies, Technologies and Applications, 205-210.

Mary, G. (1983): Evolución del margen costero de la Cordillera Cantábrica en Asturias desde el Mioceno (Evolution of the coastal margin of the Cantabrian Mountains in Asturias since Miocene). Trabajos de Geología 13, 3-35.

Ramsay, J.G. (1967): Folding and fracturing of rocks. Mc Graw-Hill, New York, 568 pp.

Ramsay, J.G. and Huber, M.I. (1987): The techniques of modern structural geology. Volume 2: folds and fractures. Academic Press, London, 309-700.

Rieke-Zapp, D.H., Rosenbauer, R. and Schlunegger, F. (2009): A photogrammetric survey-ing method for field applications. The Photogrammetric Record 24 (125), 5-22.

Suárez Vega, L.C. (1974): Estratigrafía del Jurásico de Asturias (Stratigraphy of the Jurassic of Asturias). Cuadernos de Geología Ibérica 3, 1-369.

Triggs, B., McLauchlan, P., Hartley, R. and Fitzgibbon, A. (2000): Bundle adjustment – A modern synthesis. In: Triggs, B.; Zisserman, A. and Szeliski, R. (Eds.) Vision Algorithms: Theory and Practice. Springer-Verlag, Berlin, 298-372.

Valenzuela, M.; García-Ramos, J.C. y Suárez de Centi, C. (1986): The Jurassic sedimentation in Asturias (N Spain). Trabajos de Geología 16, 121-132.

Wilson, G. (1967): The geometry of cylindrical and conical folds. Proceedings of the Geologists'
    Association 78 (1), 179–209.

Xu, X., Bhattacharya, J.P., Davies, R.K. and Aiken, C.L.V. (2001): Digital geologic zap-ping of the
    Ferron Sandstone, Muddy Creek, Utah, with GPS and reflectorless laser rangefinders. GPS
    Solutions 19 (1), 15-23.

Figure captions

Figure 1. Flux diagram showing the main steps of the proposed methodology.

Figure 2. Sketch showing how the photographs for each stereo pair should be taken. The camera is translated parallel to the outcrop trying to introduce no rotation and keeping the shooting direction constant. The procedure is repeated until the whole outcrop is covered.

Figure 3. Screen capture showing the identification of: a) targets, b) natural control points.

Figure 4. Stereoscopic pair of photographs processed with the HDR technique of a part of the cliffs at La Conejera Inlet built using the reference points obtained in the field.

Figure 5. Stereoscopic pair of photographs of a portion of the cliffs at La Conejera Inlet interpreted from a geological point of view (beds and faults) with the software Visage.

Figure 6. Structural sketch of the Permo-Mesozoic Asturian Basin indicating the situation of the studied zone (red circle), modified from Alonso et al. (2009).

Figure 7. a) Oblique photograph and b) orthophotograph of the cliffs at La Conejera Inlet where the folded and faulted Jurassic materials depicted in the geological cross-section constructed with the presented methodology crop out. The red line in figure b indicates the zone in which the studied structures crop out.

Figure 8. Equal area projection of the: a) most recent fold axes (red), and b) of the older, more important normal faults (blue) and the younger, reverse faults related to folds (black) and their associated slickensides (red).

Figure 9. Equal area projection of the poles of stratification and planes of best cylindrical fit for the northwestern sector (a) and the southeastern one (b).

Figure 10. Equal area projection of the fold axes (red), the slickensides of reverse faults (light blue) and those of normal faults (dark blue), and the planes chosen for the construction of the geological cross-sections.

Figure 11. Scheme showing how the geological interpretation on the stereoscopic pairs was projected onto the planes that constitute the geological cross-section, taking into account the fold axes and the kinematic indicators. View from above (a) and from the NE (b).

Figure 12. Cross-section of the cliff at La Conejera Inlet obtained via the strategy introduced in this work.

Table captions

Table 1. Example of resolutions achieved using the camera employed in our project (focal length: 7485; 3648 x 3276 pixels resolution) shooting from different distances and with diverse baselines.

Table 2. Voxel sizes and errors for the different pairs employed to construct the geological cross-section. The pairs are sorted from Northwest to Southeast.
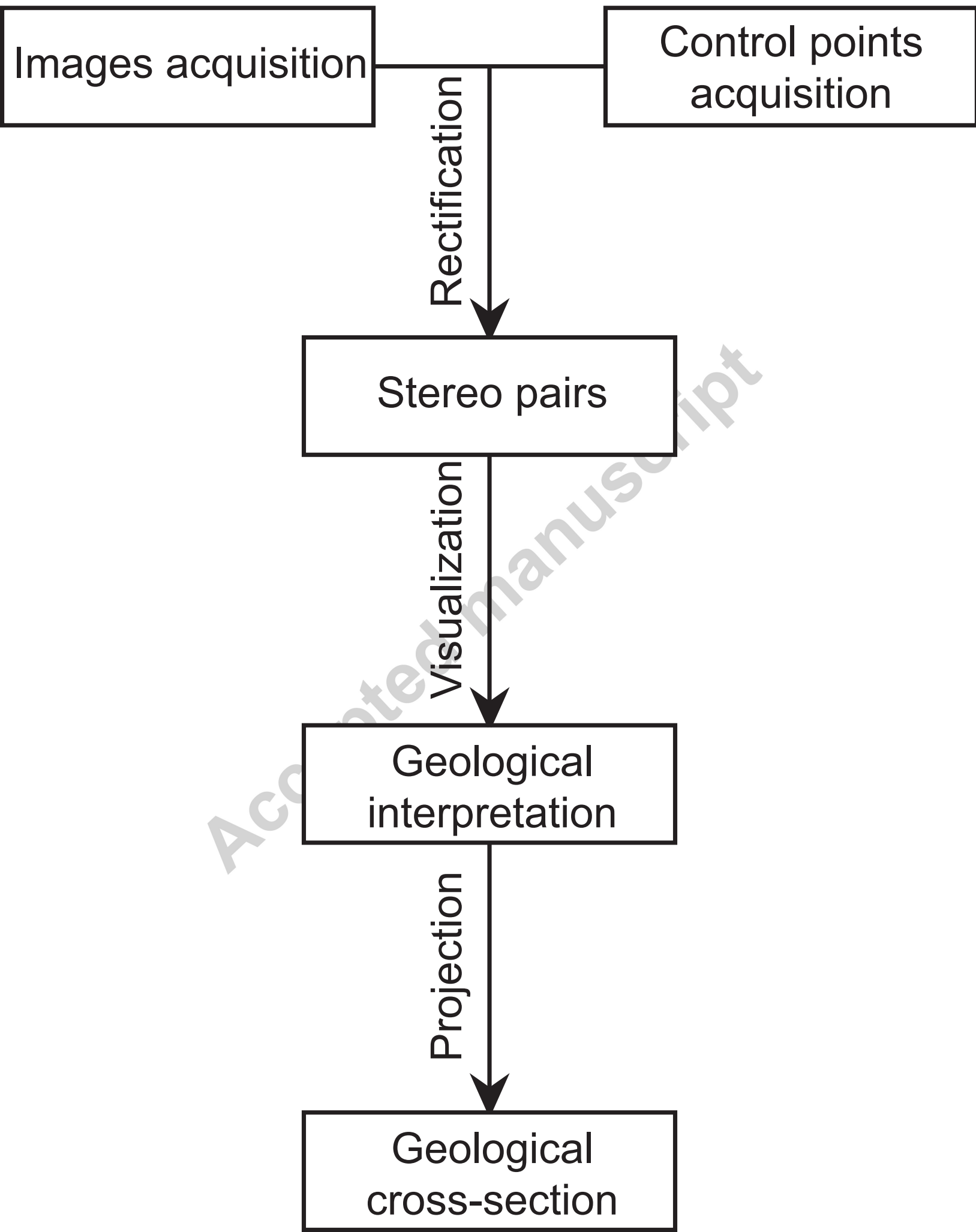
Distance (mm)	Baseline (mm)	Width-height resolution (mm)	Depth resolution (mm)
5000.0	1000.0	0.7	3.3
5000.0	1500.0	0.7	2.2
5000.0	2000.0	0.7	1.7
10000.0	2000.0	1.3	6.7
10000.0	3000.0	1.3	4.5
10000.0	4000.0	1.3	3.3
20000.0	4000.0	2.7	13.4
20000.0	6000.0	2.7	8.9
20000.0	8000.0	2.7	6.7

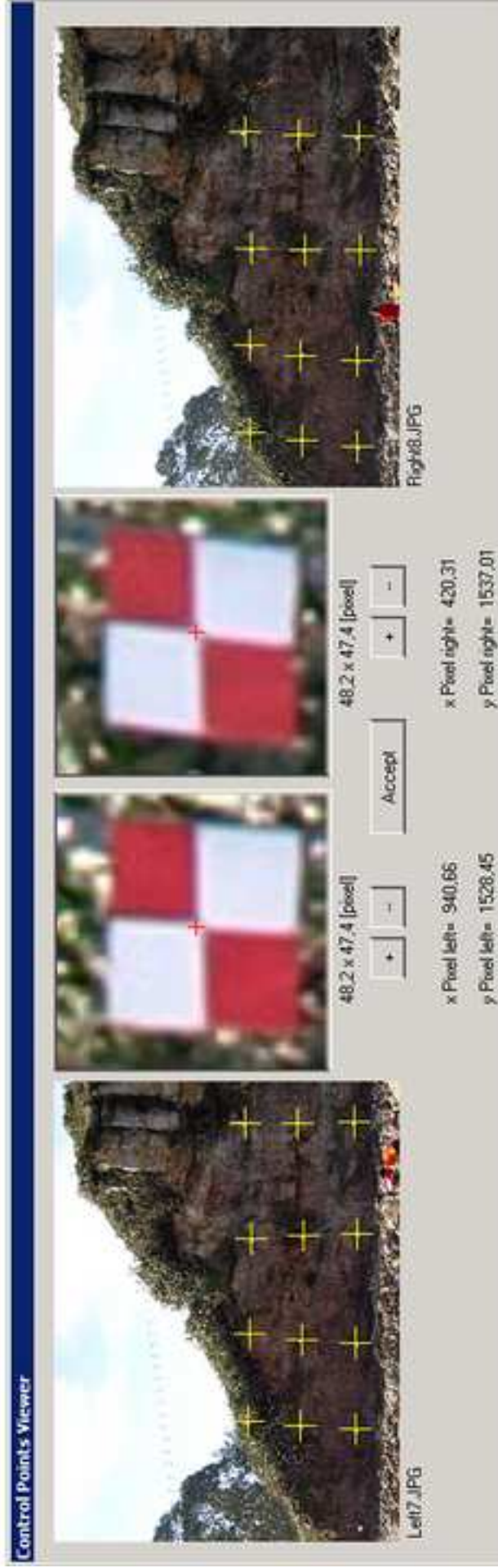|	Voxel size (mm)			Coordinates comparison (mm)		Residual transverse parallax (pixels)	
Pair	XY	Z	Diagonal	RMSD	AAD	RMSD	AAD
1	4.0	21.9	22.6	214.2	52.4	1.7	0.8
2	4.7	40.9	41.4	127.5	44.0	1.0	0.5
3	5.3	53.5	54.0	67.5	27.8	0.3	0.2
4	5.3	50.9	51.5	118.7	29.6	1.0	0.6
5	7.3	67.4	68.2	255.5	82.5	0.9	0.5
6	8.0	54.7	55.8	79.6	27.9	0.7	0.4
7	5.3	31.9	32.8	74.9	27.4	1.0	0.6
8	9.4	59.5	61.0	97.3	17.1	1.1	0.5
9	8.7	57.6	58.9	213.9	72.3	1.4	0.7
10	11.4	64.4	66.3	126.3	41.0	0.9	0.4
11	11.4	91.9	93.3	173.3	74.7	1.0	0.5
12	8.7	62.7	64.0	180.8	28.7	1.6	0.3
All	-	-	-	159.3	45.5	1.1	0.5

Highlights:

-We present a methodology for the construction of geological cross-sections.

-This methodology is based on the interpretation of stereoscopic pairs of photographs.

-It allows the creation of distortion-free geological cross-sections.

-It may be applied to cliffs, mountains slopes, trenches or similar outcrops.

-It has been successfully employed to a natural example of inversion tectonics.
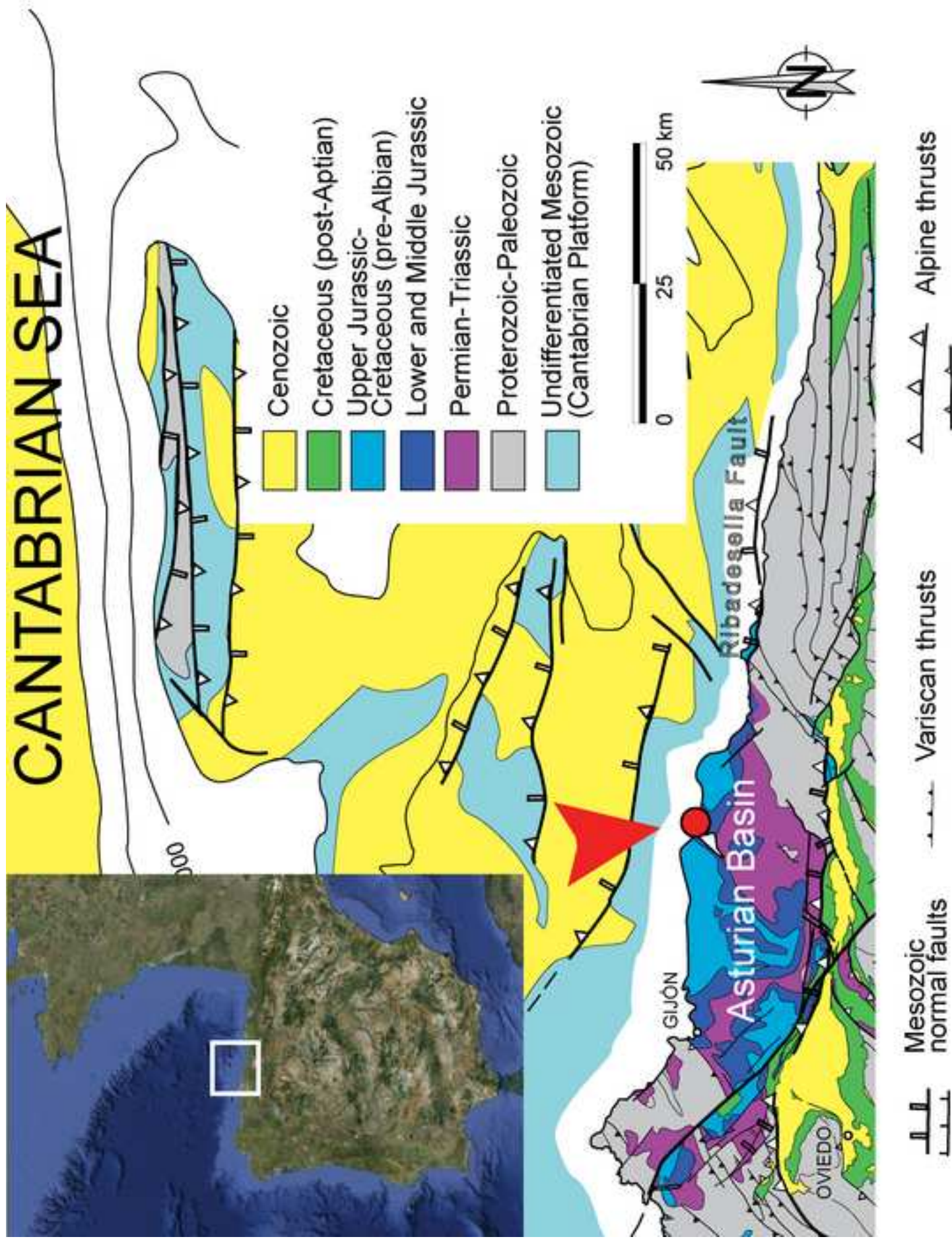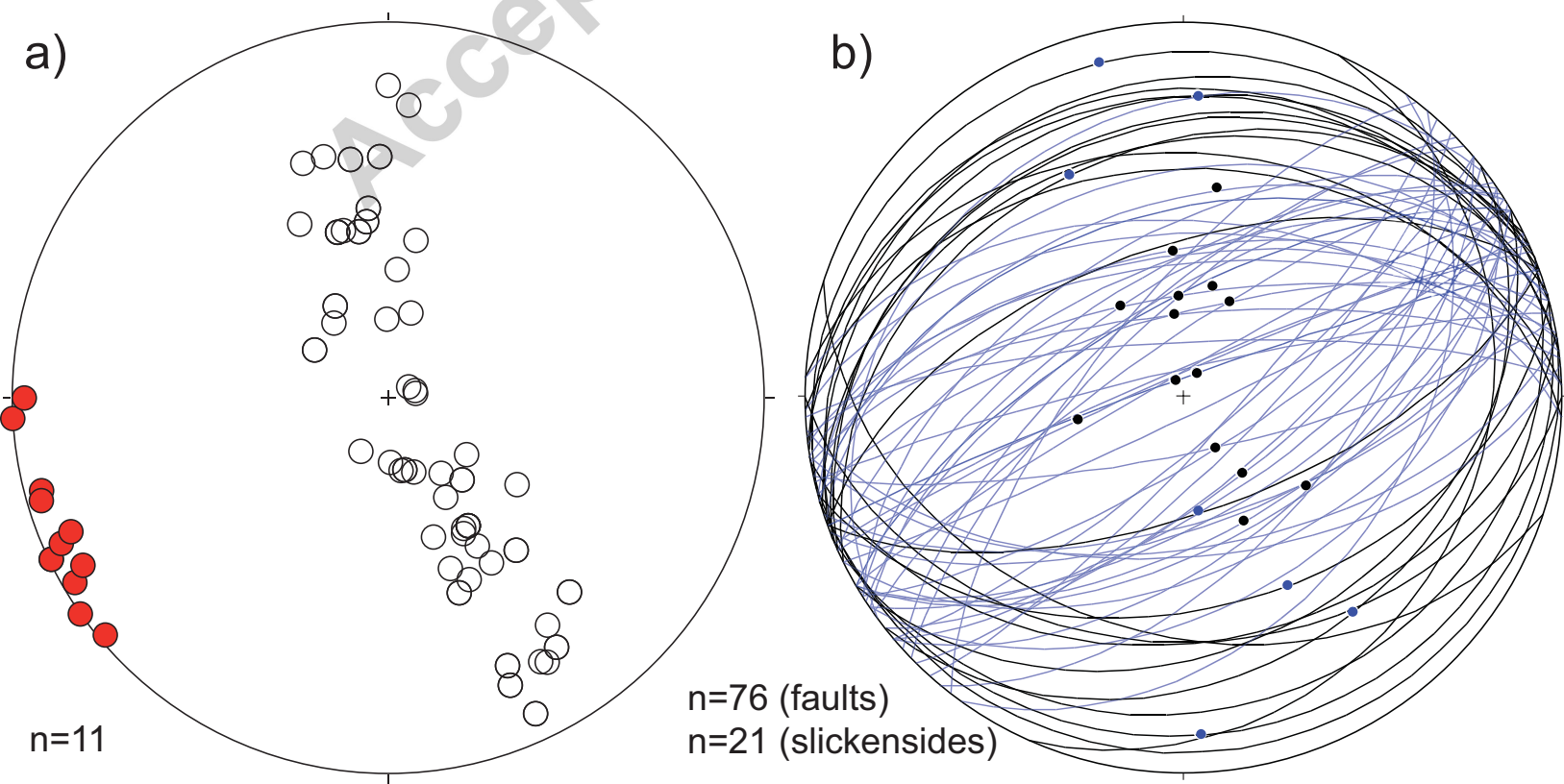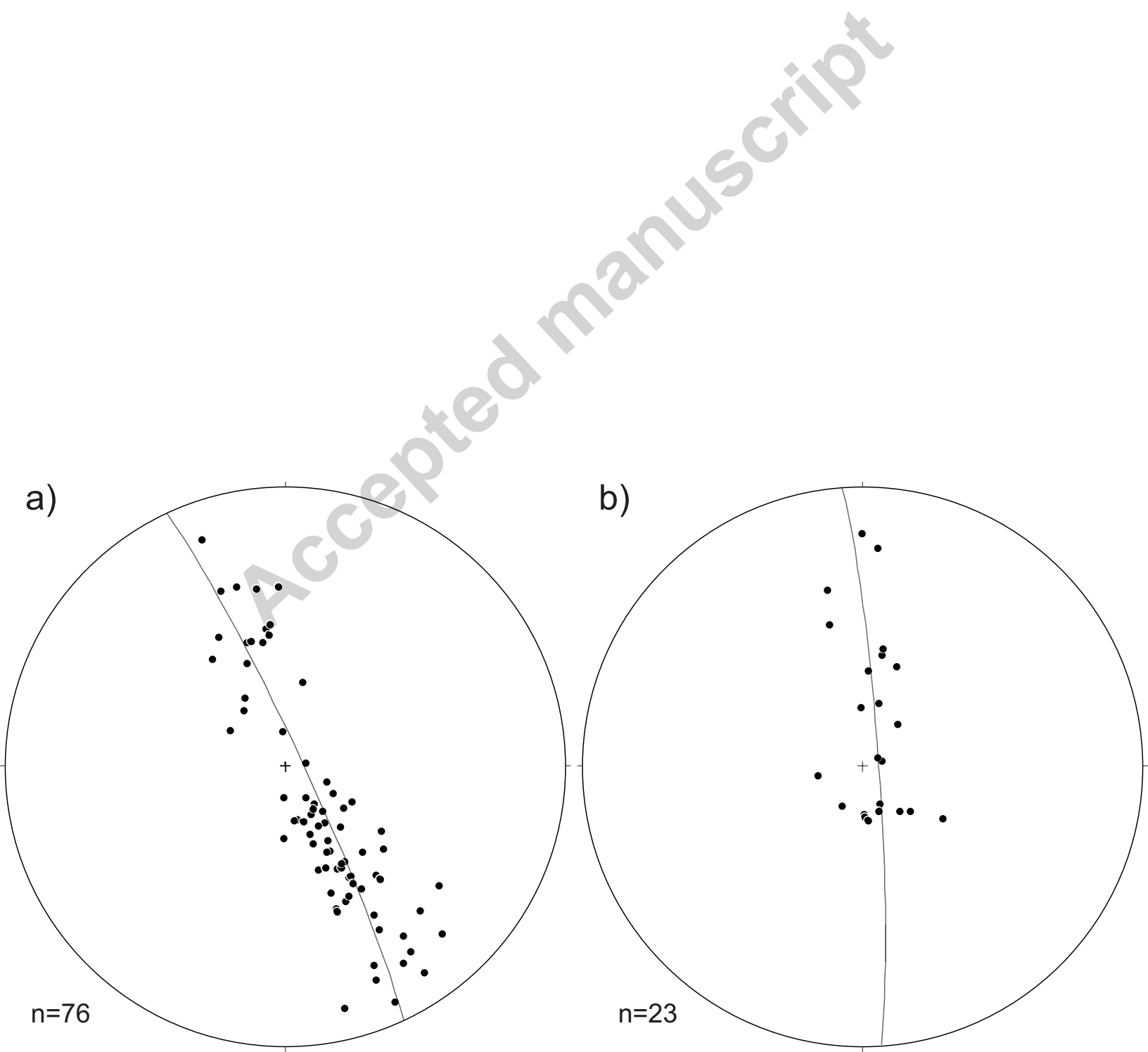
Figure 1

Figure 2

Figure 3

CANTABRIAN SEA

GIJÓN

Asturian Basin

Ribadesella Fault

OVIEDO

Legend:
- Cenozoic
- Cretaceous (post-Aptian)
- Upper Jurassic-Cretaceous (pre-Albian)
- Lower and Middle Jurassic
- Permian-Triassic
- Proterozoic-Paleozoic
- Undifferentiated Mesozoic (Cantabrian Platform)

Mesozoic normal faults

Variscan thrusts

Alpine thrusts

0   25   50 km

Figure 6

Figure 7

Figure 8

a)

n=11

b)

n=76 (faults)
n=21 (slickensides)

Figure 9

a)

n=76

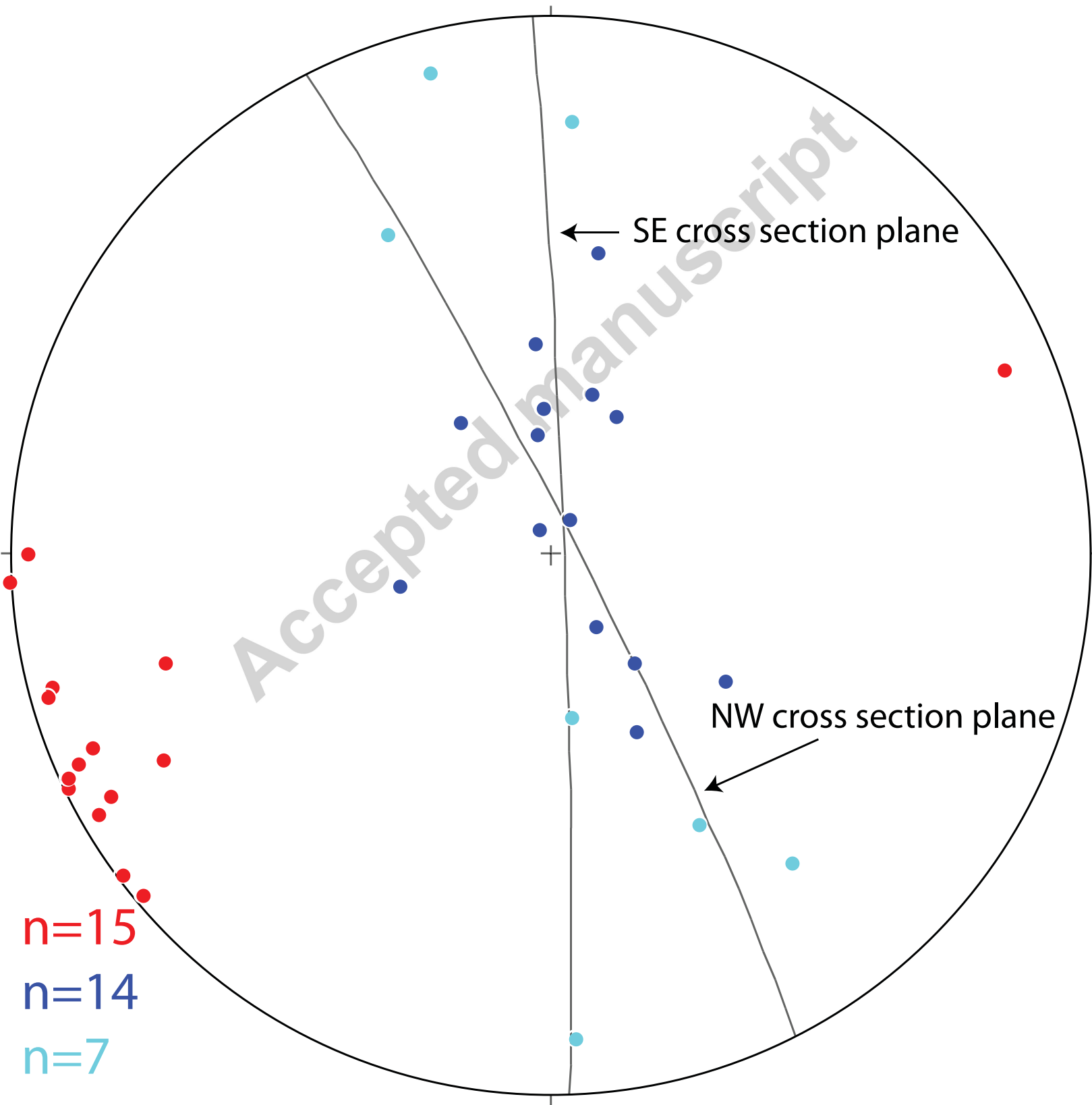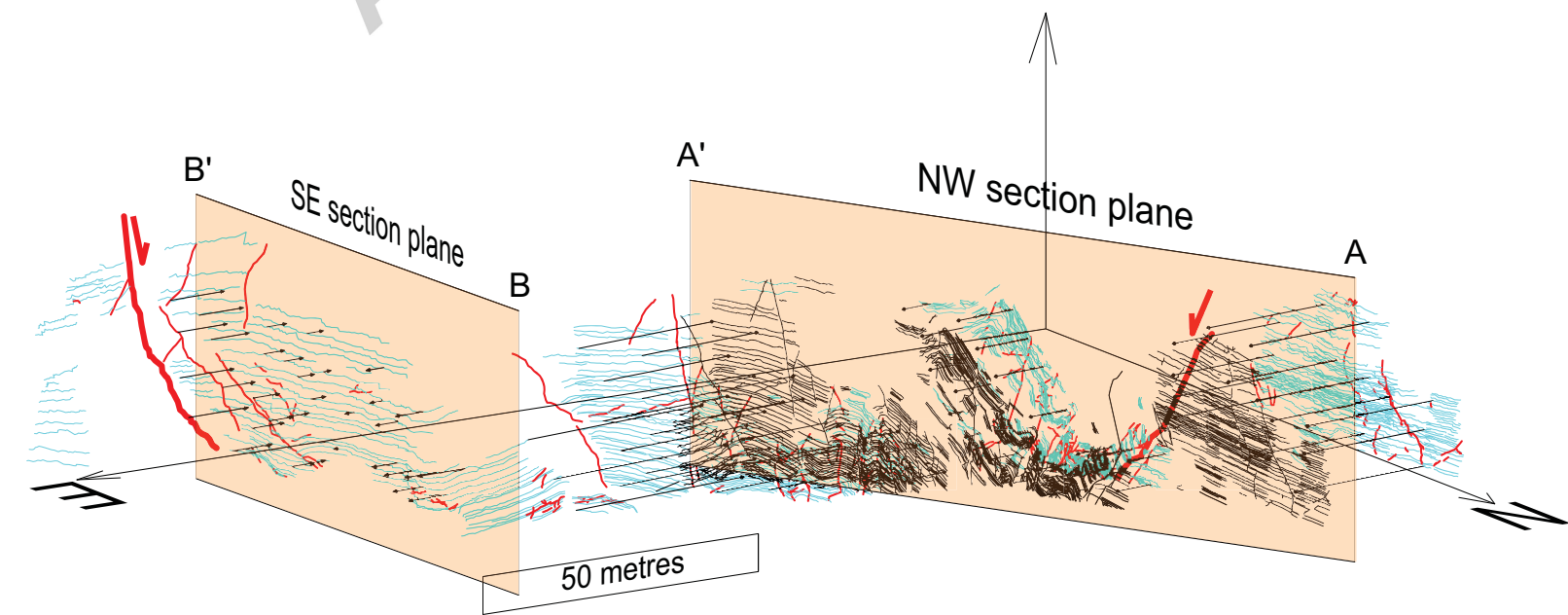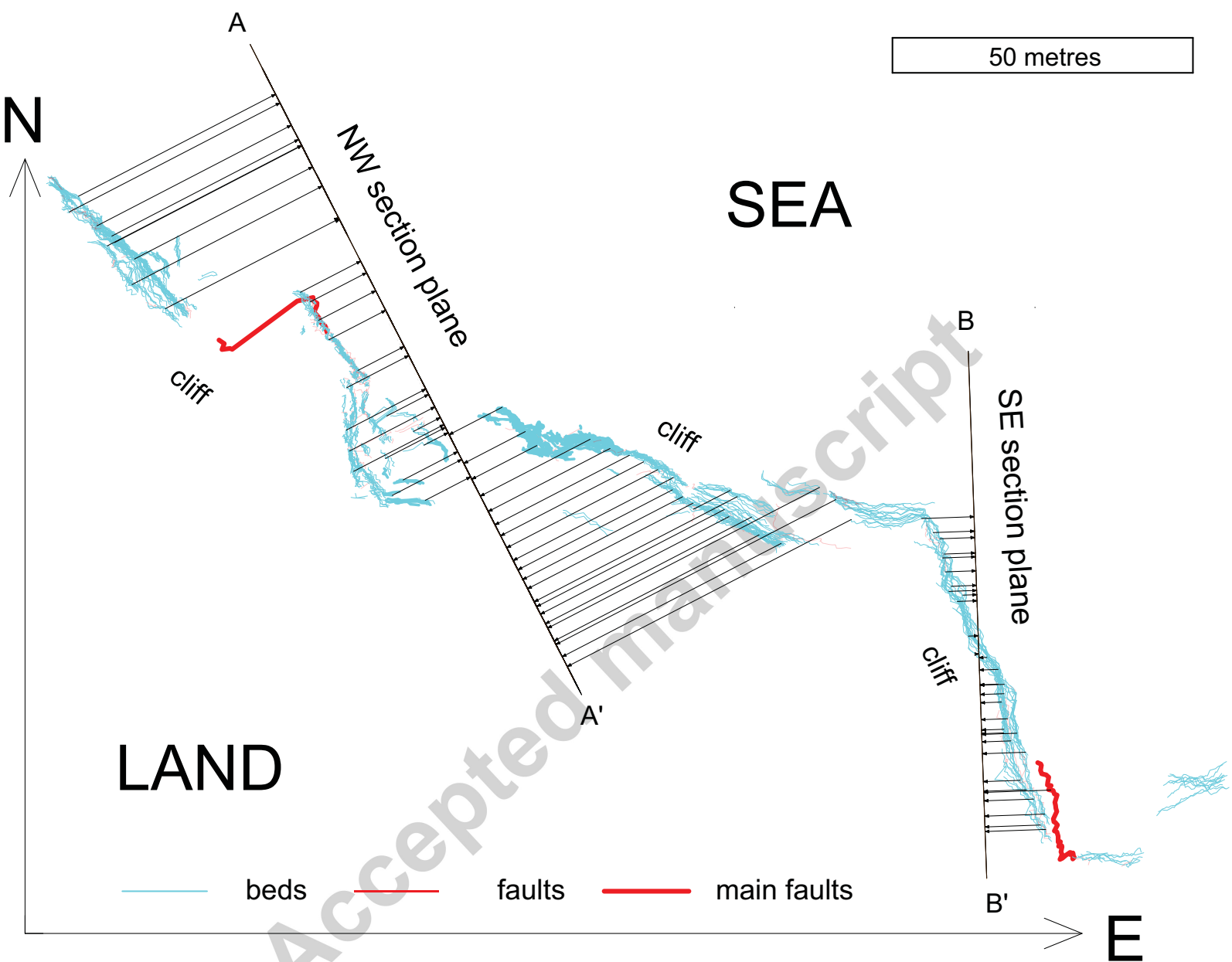b)

n=23

Figure 10

SE cross section plane

NW cross section plane

n=15

n=14

n=7

Figure 11 ACCEPTED MANUSCRIPT

Figure 12

SE

NW

Santa Mera Mb.

Buerres Mb.

Buerres Mb.

beds — faults — main faults 20 metres

B' SE section plane B A' NW section plane A